

Pulsed dipole radiation in a transformation-optics wedge waveguide designed by azimuthal space compression

Heungjoon Kim,¹ Seung Pil Pack,² Yun Yi,¹ and Hwi Kim^{1,*}

¹Department of Electronics and Information Engineering, College of Science and Technology, Korea University, Sejong Campus, Sejong-ro 2511, Sejong 339-700, South Korea

²Department of Biotechnology and Bioinformatics, Korea University, Sejong Campus, Sejong-ro 2511, Sejong 339-700, South Korea

*hwikim@korea.ac.kr

Abstract: A transformation-optics wedge waveguide designed for the simultaneous collection and directional collimation of pulsed dipole radiation is described and tested with numerical simulation. Azimuthal compression of free space toward a narrow fan-shaped waveguide sector allows dipole pulse radiation in free space to be transformed into a directional non-dispersive pulse propagating within that sector. The collection and collimation ability of the proposed structure is compared with classical approaches using metallic wedge mirrors and parabolic mirrors, which inherently allow multiple internal reflections and thus generate significant pulse distortion and low light-collection efficiency. It is shown that the optical pulse generated by the dipole and propagated through the proposed transformation-optics waveguide maintains its original shape within the structure, and demonstrates enhanced optical power.

©2013 Optical Society of America

OCIS codes: (080.2710) Inhomogeneous optical media; (220.2740) Geometric optical design; (260.1180) Crystal optics; (260.2110) Electromagnetic optics.

References and links

1. J. L. O'Brien, A. Furusawa, and J. Vučković, "Photonic quantum technologies," *Nat. Photonics* **3**(12), 687–695 (2009).
2. A. J. Shields, "Semiconductor quantum light sources," *Nat. Photonics* **1**(4), 215–223 (2007).
3. K. G. Lee, X. W. Chen, H. Eghlidi, P. Kukura, R. Lettow, A. Renn, V. Sandoghdar, and S. Götzinger, "A planar dielectric antenna for directional single-photon emission and near-unity collection efficiency," *Nat. Photonics* **5**(3), 166–169 (2011).
4. N. Gregersen, P. Kaer, and J. Mørk, "Modeling and design of high-efficiency single-photon sources," *IEEE Sel. Top. Quantum Electron.* **19**(5), 9000516 (2013).
5. Y. Ebenstein and L. A. Bentolila, "Single-molecule detection: Focusing on the objective," *Nat. Nanotechnol.* **5**(2), 99–100 (2010).
6. S. McDaniel and S. Blair, "Increased OLED radiative efficiency using a directive optical antenna," *Opt. Express* **18**(16), 17477–17483 (2010).
7. T. H. Taminiau, F. D. Stefani, F. B. Segerink, and N. F. Van Hulst, "Optical antennas direct single-molecule emission," *Nat. Photonics* **2**(4), 234–237 (2008).
8. W. Y. Liang, J. W. Dong, and H. Z. Wang, "Directional emitter and beam splitter based on self-collimation effect," *Opt. Express* **15**(3), 1234–1239 (2007).
9. R. Zhou, X. Chen, and W. Lu, "Strong focusing properties and far-field focus in the two-dimensional photonic-crystal-based concave lens," *Phys. Rev. E Stat. Nonlin. Soft Matter Phys.* **74**(1), 016610 (2006).
10. O. Kidwai, S. V. Zhukovsky, and J. E. Sipe, "Dipole radiation near hyperbolic metamaterials: applicability of effective-medium approximation," *Opt. Lett.* **36**(13), 2530–2532 (2011).
11. E. M. Purcell, "Spontaneous emission probabilities at radio frequencies," *Phys. Rev.* **69**, 681 (1946).
12. E. Yablonovitch, "Inhibited Spontaneous Emission In Solid-State Physics And Electronics," *Phys. Rev. Lett.* **58**(20), 2059–2062 (1987).
13. D. Schurig, J. B. Pendry, and D. R. Smith, "Calculation of material properties and ray tracing in transformation media," *Opt. Express* **14**(21), 9794–9804 (2006).
14. J. B. Pendry, D. Schurig, and D. R. Smith, "Controlling electromagnetic fields," *Science* **312**(5781), 1780–1782 (2006).
15. U. Leonhardt, "Optical conformal mapping," *Science* **312**(5781), 1777–1780 (2006).

16. U. Leonhardt, "Note on conformal invisibility devices," *New J. Phys.* **8**(7), 118 (2006).
17. X. Xu, Y. Feng, Y. Hao, J. Zhao, and T. Jiang, "Infrared carpet cloak designed with uniform silicon grating structure," *Appl. Phys. Lett.* **95**(18), 184102 (2009).
18. J. Li and J. B. Pendry, "Hiding under the Carpet: A New Strategy for Cloaking," *Phys. Rev. Lett.* **101**(20), 203901 (2008).
19. M. Rahm, D. A. Roberts, J. B. Pendry, and D. R. Smith, "Transformation-optical design of adaptive beam bends and beam expanders," *Opt. Express* **16**(15), 11555–11567 (2008).
20. D.-H. Kwon and D. H. Werner, "Polarization splitter and polarization rotator designs based on transformation optics," *Opt. Express* **16**(23), 18731–18738 (2008).
21. B. Wang and K.-M. Huang, "Shaping the radiation pattern with mu and epsilon-near-zero metamaterials," *PIER* **106**, 107–119 (2010).
22. J. J. Zhang, Y. Luo, S. Xi, H. S. Chen, L. X. Ran, B.-I. Wu, and J. A. Kong, "Directive emission obtained by coordinate transformation," *PIER* **81**, 437–446 (2008).
23. P.-H. Tichit, S. N. Burokur, D. Germain, and A. de Lustrac, "Coordinate-transformation-based ultra-directive emission," *Electron. Lett.* **47**(10), 580–582 (2011).
24. D. H. Kwon and D. H. Werner, "Transformation optical designs for wave collimators, flat lenses and right-angle bends," *New J. Phys.* **10**(11), 115023 (2008).
25. D. H. Kwon and D. H. Werner, "Flat focusing lens designs having minimized reflection based on coordinate transformation techniques," *Opt. Express* **17**(10), 7807–7817 (2009).
26. M. Schmiele, V. S. Varma, C. Rockstuhl, and F. Lederer, "Designing optical elements from isotropic materials by using transformation optics," *Phys. Rev. A* **81**(3), 033837 (2010).
27. J. P. Turpin, A. T. Massoud, Z. H. Jiang, P. L. Werner, and D. H. Werner, "Conformal mappings to achieve simple material parameters for transformation optics devices," *Opt. Express* **18**(1), 244–252 (2010).

1. Introduction

The collection and collimation of optical radiation from dipole quantum emitters has been an important subject for practical application as well as fundamental research. The efficient collection of dipole radiation is critical to optical and quantum information processing [1–4], biophotonics [5], displays [6], and nanophotonics [7]. To achieve high collection efficiency, the accurate and consistent collimation of dipole radiation is required, and this is currently considered a fundamental technological obstacle.

Indeed, the classical approaches for collecting and collimating optical dipole radiation are limited in their efficiency (Fig. 1).

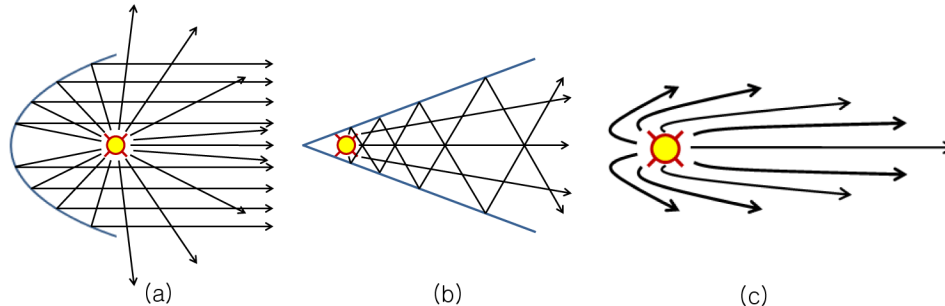


Fig. 1. Classical approaches for collecting dipole radiation using (a) a parabolic mirror, and (b) a wedge mirror waveguide; compared with (c) ideal dipole collection and collimation

As seen in Fig. 1(a), a simple parabolic mirror can reflect in a specified direction the radiation emitted from one side of a central dipole placed at the focal point of the mirror. However, a considerable portion of the radiation on the other side of the source inevitably leaks past the mirror, resulting in a collimation efficiency of less than 50%. In Fig. 1(b), a wedged waveguide structure with a highly reflective internal surface can be used to reform the dipole radiation into unidirectional radiation. In this situation, waveguide dispersion can be significant due to multiple reflections within the wedge, and thus diode radiation with a very short pulse width and a wide spectral bandwidth cannot maintain its shape during propagation. It is clear from these two examples that the collimation of bidirectional radiation is a challenging problem. Figure 1(c) presents an ideal situation for the collection and

collimation of optical dipole radiation. The optical rays radiated toward the left reverse direction and become perfectly collimated in the specified direction with little divergence.

Recently novel approaches based on photonic crystals [8, 9], plasmonics and metamaterials [10] have been actively explored to provide creative solutions for the manipulation of dipole radiation. In photonic crystal cavities, the self-collimation effect of optical dipole radiation embedded in the cavities has been observed. Theoretically, this effect can be used to collimate the dipole radiation and transform it into a directional plane wave. Furthermore, the amount of radiative emissions can be enhanced in the cavity structures by the Purcell effect [11, 12]. In theoretical photonics, transformation optics pursues a radically different approach to many non-classical optical design problems based on the invariance of Maxwell's equations under coordinate-transformation [13]. Indeed, after initially proposing the perfect lens and an invisibility cloak [14–16], the fields of transformation optics and metamaterials have expanded fast. As a result, a variety of unconventional optical designs, such as the carpet cloak [17, 18], lossless beam bending devices [19] and polarization controllers [20], have been reported.

Several promising proposals based on transformation optics that address the problem of dipole radiation have been reported, with noticeable examples as directional antennas [21–23], flat focus lenses [24, 25], and quad-beam cylindrical-to-plane wave converters [26, 27]. In most of the previous research, a continuous wave (CW) was assumed and bidirectional collimation was adopted as the main collimation scheme.

In this paper, we propose a novel transformation-optics waveguide structure that can near perfectly collect optical dipole radiation and transfer it unidirectionally, similar to the ideal case presented in Fig. 1(c). For convenience, a two-dimensional (2D) structure for a 2D dipole radiation source is investigated with a COMSOL multiphysics simulator and assuming that the permittivity and permeability of the metamaterial structure obtained are nearly constant for the bandwidth of a femtosecond pulse, we analyze dipole pulse generation and propagation in the proposed waveguide structure and contrast its performance with that of classical structures.

This paper is organized as follows. In Section 2, the design of the proposed transformation-optics dipole collimation structure is described. In Section 3, the collimation characteristics of a classical wedge mirror and the proposed structure are comparatively analyzed.

2. The design of the transformation-optics wedge waveguide

The design objective for the waveguide is to efficiently extract a unidirectional and spatially collimated pulsed dipole field without the pulse distortion due to waveguide dispersion. The main idea is that the azimuthal space compression transforms pulsed dipole radiation in the original space to a highly collimated non-dispersive pulse in the transformed space. The resultant optical structure in the transformed space is referred to as the transformation-optics wedge waveguide. The design concept is illustrated in Fig. 2.

In Fig. 2(a), the negative real axis is indicated by a bolded red line splitting the free space into upper ($y' \geq 0$) and lower ($y' < 0$) areas in the negative x' -region. The upper and lower areas are azimuthally compressed in clockwise and counter-clockwise directions, respectively. The coordinate transformation represented in Fig. 2 is mathematically described by the following transformation function:

$$r'(r, \phi, z) = r, \quad (1a)$$

$$\phi'(r, \phi, z) = \begin{cases} -\beta + (\phi + \alpha)(180 - \beta) / (180 - \alpha) & \text{for } -180^\circ \leq \phi \leq -\alpha^\circ \\ \phi\beta / \alpha & \text{for } -\alpha^\circ \leq \phi \leq \alpha^\circ \\ \beta + (\phi - \alpha)(180 - \beta) / (180 - \alpha) & \text{for } \alpha^\circ \leq \phi \leq 180^\circ \end{cases}, \quad (1b)$$

$$z'(r, \phi, z) = z, \quad (1c)$$

where α and β are the central azimuthal angles of the wedge waveguide defined in the original space and in the transformed space, respectively.

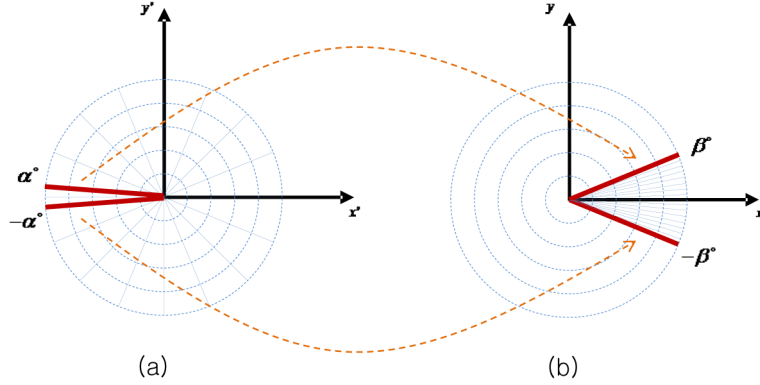


Fig. 2. Geometries of the transformation-optics wedge waveguide for optical dipole collimation in (a) the original space, and (b) the transformed space

Let β be termed the compression parameter. In transformation optics, the permittivity and permeability functions in transformed space are given respectively by:

$$\boldsymbol{\varepsilon}' = \mathbf{J} \cdot \boldsymbol{\varepsilon} \cdot \mathbf{J}^T / \det(\mathbf{J}), \quad (2a)$$

$$\boldsymbol{\mu}' = \mathbf{J} \cdot \boldsymbol{\mu} \cdot \mathbf{J}^T / \det(\mathbf{J}), \quad (2b)$$

where $\boldsymbol{\varepsilon}$ and $\boldsymbol{\mu}$ are the permittivity and permeability tensors in the original space, and $\boldsymbol{\varepsilon}'$ and $\boldsymbol{\mu}'$ are the permittivity and permeability tensors in the transformed space. \mathbf{J} is the Jacobian tensor represented as:

$$\mathbf{J} = \begin{pmatrix} \partial r' / \partial r & \partial r' / \partial \phi & \partial r' / \partial z \\ \partial \phi' / \partial r & \partial \phi' / \partial \phi & \partial \phi' / \partial z \\ \partial z' / \partial r & \partial z' / \partial \phi & \partial z' / \partial z \end{pmatrix}. \quad (3a)$$

By substituting Eqs. (1a)-(1c) into Eq. (3a), we can obtain the Jacobian tensor as:

$$\mathbf{J} = \begin{pmatrix} 1 & 0 & 0 \\ 0 & p_i & 0 \\ 0 & 0 & 1 \end{pmatrix}, \quad (3b)$$

where p_i is defined by:

$$p_i = \begin{cases} \beta / \alpha & \text{for } i = 1 \\ (180 - \beta) / (180 - \alpha) & \text{for } i = 2 \end{cases} \quad (3c)$$

and p_1 and p_2 correspond to the azimuthally compressed and expanded regions respectively. The obtained permittivity and permeability tensors take the form of:

$$\boldsymbol{\varepsilon}' / \varepsilon_0 = \boldsymbol{\mu}' / \mu_0 = \begin{pmatrix} 1 / p_i & 0 & 0 \\ 0 & p_i & 0 \\ 0 & 0 & 1 / p_i \end{pmatrix}. \quad (4)$$

The permittivity and permeability tensors are described in the cylindrical coordinate system, which can be expressed through vector representation in the Cartesian coordinate system as:

$$\begin{pmatrix} A_\rho \\ A_\phi \\ A_z \end{pmatrix} = \begin{pmatrix} \cos \phi & \sin \phi & 0 \\ -\sin \phi & \cos \phi & 0 \\ 0 & 0 & 1 \end{pmatrix} \begin{pmatrix} A_x \\ A_y \\ A_z \end{pmatrix} = \mathbf{T}_{cr} \begin{pmatrix} A_x \\ A_y \\ A_z \end{pmatrix}. \quad (5)$$

From Eq. (5), the electric displacement vector \mathbf{D}_r in the Cartesian coordinate system is given by the constitutive relation:

$$\mathbf{D}_r = \mathbf{T}_{cr}^{-1} \cdot \boldsymbol{\epsilon}' \cdot \mathbf{T}_{cr} \mathbf{E}_r. \quad (6)$$

From Eqs. (4)-(6), the permittivity and permeability profiles for the above transformation of the proposed dipole collimator are obtained by:

$$\boldsymbol{\epsilon}'_r / \epsilon_0 = \boldsymbol{\mu}'_r / \mu_0 = \begin{pmatrix} \epsilon_{xx} & \epsilon_{xy} & 0 \\ \epsilon_{yx} & \epsilon_{yy} & 0 \\ 0 & 0 & \epsilon_{zz} \end{pmatrix} = \begin{pmatrix} (1/p_i) \cos^2 \phi + p_i \sin^2 \phi & (1/p_i - p_i) \cos \phi \sin \phi & 0 \\ (1/p_i - p_i) \cos \phi \sin \phi & (1/p_i) \sin^2 \phi + p_i \cos^2 \phi & 0 \\ 0 & 0 & 1/p_i \end{pmatrix}. \quad (7)$$

In Fig. 3, the components of the anisotropic permittivity tensor with $\alpha = 179.9^\circ$ and $\beta = 10^\circ$ are plotted. It is seen that the permittivity tensor profiles in the expanded area are anisotropic and inhomogeneous, and, in some part in the expanded area, the permittivity magnitude is much larger than that in the compressed area. Also, if a cone-shaped gap in the original space is expanded three-dimensionally, the other space can be compressed to three-dimensional cone-shaped waveguide structure, which means that the proposed design concept can be straightforwardly extended to three-dimensional structure.

The dipole radiation in the wedge waveguide with the designed permittivity and permeability tensor is analyzed numerically. Firstly, the continuous radiation of an electric dipole placed in free space and inside the proposed waveguide structure is simulated with a COMSOL Multiphysics simulator. The operating wavelength, the radius of the structure and the thickness of the circular perfect-matched-layer (PML) are set to $\lambda = 633\text{nm}$, $R = 17\lambda$, and $t_{PML} = 3\lambda$, respectively. The optical field distributions from an electric dipole in free space and the proposed structure are presented in Figs. 4(a) and 4(b), respectively.

In the case of free space radiation, a dipole radiation with transversal electric (TE) polarization is excited at the position $(x, y) = (0, 0)$. In the case of the proposed structure, the dipole is located at $(x, y) = (\Delta x, 0)$, which is a position with a slight deviation from the origin to prevent singular problem in numerical analysis. In Fig. 4(b), the electric field distribution in the proposed waveguide guide with $\beta = 10^\circ$ and $\alpha = 179.9^\circ$ is presented. Figure 4(b) confirms that the electric field is tightly confined in the compressed region. In Figs. 4(c) and 4(d), the time-averaged power flow distribution in the cross-section of the waveguide and the spatial average power is plotted with respect to the angle α .

As shown in Fig. 4(c), the output power flow in the expanded region is inversely proportional to the magnitude of α . Actually, Fig. 4(c) is the magnitude plot of the Poynting vector and the inset in Fig. 4(c) is the directional plot of the magnitude-normalized vectors. Therefore, in the expanded region, the vector flows in the inset are perceived, but we should see the magnitude plot of the Poynting vector in the expanded region is very small. In the perfect matched layer (PML), the direction vectors are perceived, but their real magnitude are negligible.

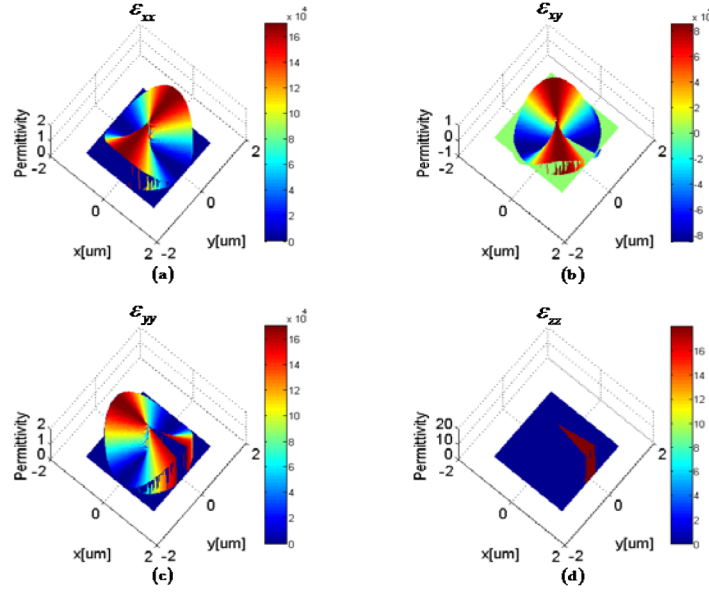


Fig. 3. Spatial distribution of permittivity: (a) ϵ_{xx} , (b) ϵ_{xy} , (c) ϵ_{yy} and (d) ϵ_{zz} .

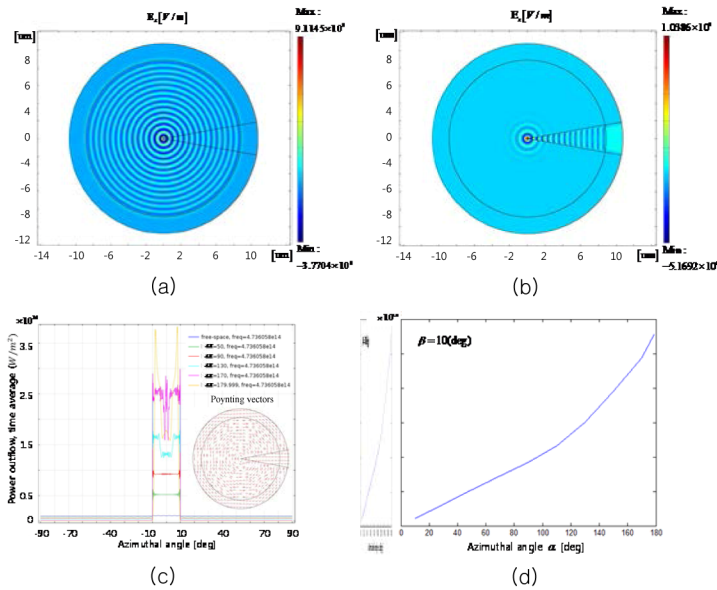


Fig. 4. Comparison of continuous dipole radiation waves in (a) free space, and (b) in the proposed dipole collimating structure with $\alpha = 179.9^\circ$. (c) Spatial time-averaged power flow distribution and (d) the spatial average of the power flow in the compressed region for various α .

The optical power flow near the boundary is slightly greater than the optical power flow in the center region of the waveguide. Interesting features of the Poynting vector distribution are visualized in Fig. 4(c). In the expanded region, the Poynting vectors are rotated around the center of the dipole position, meaning that photons emitted outside the waveguide complete a round-trip and return to the symmetric point at the opposite side wall. All photons radiated from the dipole source are directed along the waveguide channel. In Fig. 4(d), it is seen that

as the compression parameter α increases, the optical power in the compressed wedge waveguide region is enhanced.

3. Pulsed dipole radiation in the wedge waveguide

In this section, the pulsed dipole radiation in the proposed structure is simulated. The basic assumption in this analysis is that in the spectral band of femtosecond pulses with center wavelength of $\lambda = 633\text{nm}$, the permittivity and permeability tensors are non-dispersive. Then the tensor profiles in Fig. 3 are not dependent on the frequency components within the spectral band of the femtosecond pulses.

When the electric dipole generates pulsed radiation in free space, the electric field propagates with radial symmetry as shown in Fig. 5(a), which presents four snapshots of the pulsed dipole radiation from an electric dipole placed at $(x, y) = (0, 0)$ taken at $t = 15\text{fs}$, $t = 20\text{fs}$, $t = 25\text{fs}$, and $t = 30\text{fs}$. This propagation is represented in the space-time domain in Fig. 5(b). In free space, pulse distortion is not observed and the group velocity is the speed of light in a vacuum.

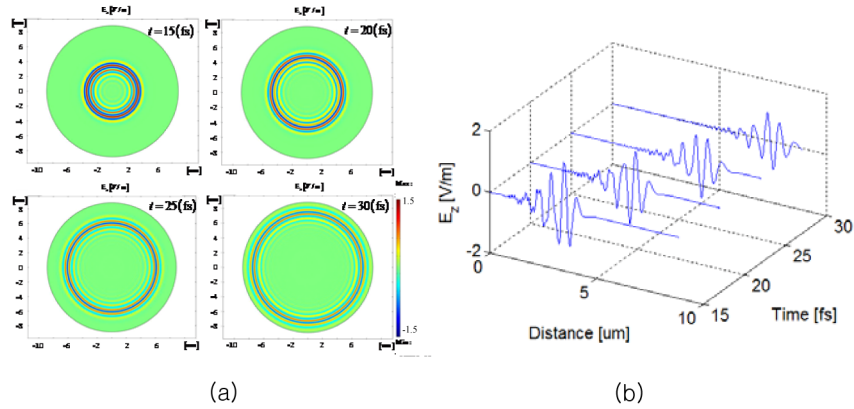


Fig. 5. Pulsed dipole radiation distributions in free space at (a) $t = 15\text{fs}$, $t = 20\text{fs}$, $t = 25\text{fs}$, and $t = 30\text{fs}$; and (b) pulse propagation in the space-time domain

In Fig. 6, snapshots of dipole radiation in the classical wedge mirror are presented. As seen in Fig. 6(b), pulse broadening is clearly observed, which is caused by multiple reflections within the wedge waveguide, i.e., the waveguide dispersion effect. The speed of pulse propagation, i.e., the group velocity, is smaller in the wedge mirror than in free space. The slow group velocity and pulse distortion are considerable features of the wedge mirror.

In contrast to the simulation results of the classical wedge structure in Fig. 6, pulse broadening does not appear in the field distribution during simulations of the proposed waveguide structure (Fig. 7). In principle, the shape of the pulse envelope is preserved inside the proposed structure just as it occurs in free space. That means that the proposed azimuthally compressed transformation-optics structure is ideal for focusing and collimating pulsed dipole radiation.

The group velocity of the classical wedge mirror waveguide is strongly dependent on waveguide geometry, itself the result of the geometric effect, i.e., waveguide dispersion. The group velocity of the proposed waveguide is constant without respect to geometry. When we consider only the geometric effect, the effect of geometric change can be completely compensated by the adaptive variation in permittivity and permeability tensors given by the design Eq. (7).

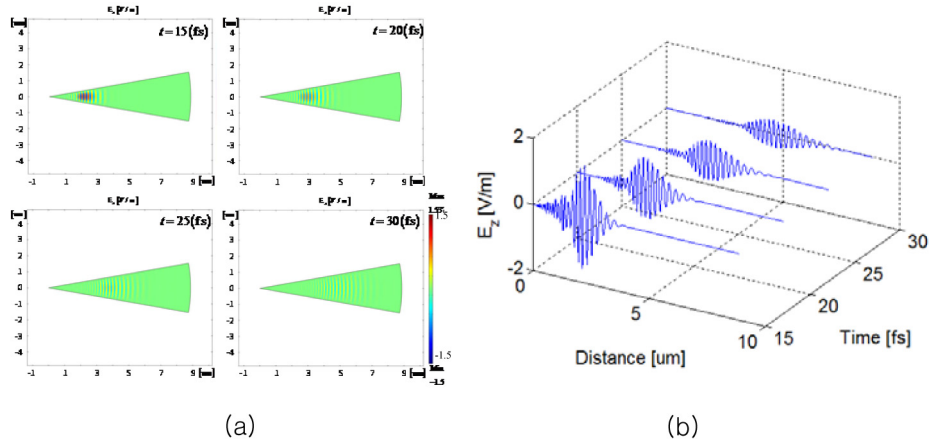


Fig. 6. Pulsed dipole radiation distribution in the classical wedge mirror at (a) $t = 15$ fs, $t = 20$ fs, $t = 25$ fs, and $t = 30$ fs and (b) pulse propagation in the space-time domain

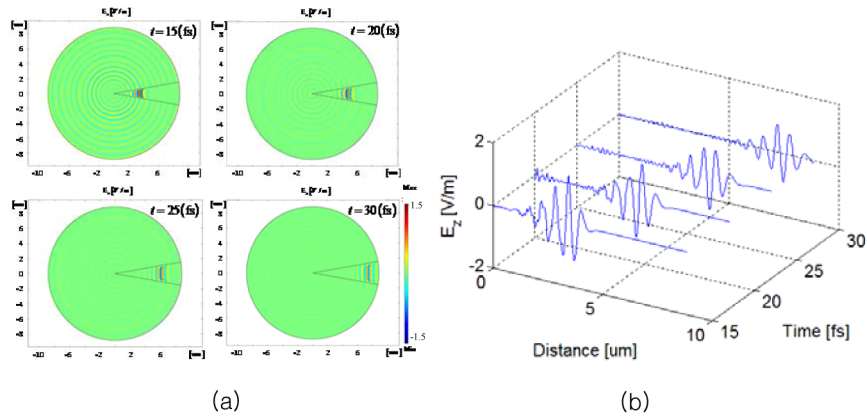


Fig. 7. Pulsed dipole radiation in the proposed dipole pulse collimator at (a) $t = 0$ fs, (b) $t = 5$ fs, (c) $t = 10$ fs, (d) $t = 15$ fs, and (e) pulse propagation in the space-time domain.

4. Conclusion

In this paper, we have proposed a transformation-optic wedge waveguide structure for the effective collection and collimation of dipole radiation. The wavefront of the pulsed dipole radiation preserves the profile of equiphase wavefront without pulse distortion, even in the narrow wave-guiding channel. This property is an improvement over the classical wedge mirror structure, which facilitates multiple internal reflections, leading to a pulse distortion. It is straightforward. Our proposed structure can be used to produce a metamaterial-based unidirectional dipole photon source for practical applications and theoretical research.

Acknowledgment

Heungjoon Kim and Seung Pil Pack both contributed equally to this paper. This research was supported by the Basic Research Program (2010-0022088) through the National Research Foundation of Korea (NRF), funded by the Ministry of Education, Science, and Technology (MEST), and supported by the Marine Biomaterials Research Center grant from the Marine Biotechnology Program funded by the Ministry of Land, Transport and Maritime Affairs, Korea.